sustainability

MDPI

Article

Simulating Potential Impacts of Future Climate Change on *Post-Rainy* Season Sorghum Yields in India

Keerthi Chadalavada [1,2], Sridhar Gummadi [3,*], Koteswara Rao Kundeti [4], Dakshina Murthy Kadiyala [5], Kumara Charyulu Deevi [2], Kailas Kamaji Dakhore [6], Ranjitha Kumari Bollipo Diana [1] and Senthil Kumar Thiruppathi [1]

1 Department of Botany, Bharathidasan University, Tiruchirappalli 620024, India; keerthichadalawada@gmail.com (K.C.); ranjithakumari2004@yahoo.co.in (R.K.B.D.); senthilbdc@bdu.ac.in (S.K.T.)
2 International Crops Research Institute for the Semi-Arid Tropics (ICRISAT), Patancheru 502324, India; d.kumaracharyulu@cgiar.org
3 CGIAR Research Program for Climate Change, Agriculture and Food Security (CCAFS), International Rice Research Institute (IRRI), IRRI-CCAFS Office, Agricultural Genetics Institute, Hanoi 03000, Vietnam
4 Center for Climate Change and Sustainability, Azim Premji University, Bengaluru 562125, India; koti.meteo@gmail.com
5 Department of Agronomy, Acharya NG Ranga Agricultural University, Guntur 522034, India; dakshu2k@gmail.com
6 All India Coordinated Research Project on Agrometeorology, Vasantrao Naik Marathwada Krishi Vidyapeeth, Parbhani 431402, India; dakhorekk@gmail.com
* Correspondence: sridhar.gummadi@irri.org

Abstract: Given the wide use of the multi-climate model mean (MMM) for impact assessment studies, this work examines the fidelity of Coupled Model Intercomparison Project Phase 5 (CMIP5) in simulating the features of Indian summer monsoons as well as the *post-rainy* seasons for assessing the possible impacts of climate change on post-rainy season sorghum crop yields across India. The MMM simulations captured the spatial patterns and annual cycles of rainfall and surface air temperatures. However, bias was observed in the precipitation amounts and daily rainfall intensity. The trends in the simulations of MMM for both precipitation and temperatures were less satisfactory than the observed climate means. The Crop Environment Resource Synthesis (CERES)-sorghum model was used to estimate the potential impacts of future climate change on post-rainy season sorghum yield values. On average, post-rainy season sorghum yields are projected to vary between −4% and +40% as well as +10% and +59% in the near future (2040–2069) for RCP 4.5 and RCP 8.5, respectively, and between +20% and +70% (RCP 4.5) as well as +38% and +89% (RCP 8.5) in the far future (2070–2099). Even though surface air temperatures are increasing in future climate change projections, the findings suggest that an increase in the post-rainy season sorghum yields was due to an increase in the rainfall amounts up to 23% and an increase in the atmospheric CO_2 levels by the end of the 21st century. The results suggest that the projected climate change during the post-rainy season over India is an opportunity for smallholders to capitalize on the increase in rainfall amounts and further increase sorghum yields with appropriate crop management strategies.

Keywords: *post-rainy* sorghum; crop simulation models; climate change impacts; crop yields

Citation: Chadalavada, K.; Gummadi, S.; Kundeti, K.R.; Kadiyala, D.M.; Deevi, K.C.; Dakhore, K.K.; Bollipo Diana, R.K.; Thiruppathi, S.K. Simulating Potential Impacts of Future Climate Change on *Post-Rainy* Season Sorghum Yields in India. *Sustainability* **2022**, *14*, 334. https://doi.org/10.3390/su14010334

Academic Editors: Baojie He, Ayyoob Sharifi, Chi Feng and Jun Yang

Received: 11 November 2021
Accepted: 14 December 2021
Published: 29 December 2021

1. Introduction

Sorghum is an important nutraceutical crop for the small and marginal farmers across the semi-arid tropics (SAT) of the world [1]. Globally, sorghum is the fifth largest cereal preferred in diverse ecologies. Primarily, the crop is cultivated in four (Asia, Africa, the Pacific and the Americas) major regions across the globe. In India, sorghum is the fourth largest cereal crop. In the case of Africa, it is the second most important crop after maize [2]. Sorghum is one of the most preferred climate-smart crops for rainfed farmers under severe

moisture stress environments. It can be grown successfully under limited soil moisture availability and with inadequate application of other inputs [3]. At present, the crop is being cultivated in both the monsoon (1.85 m ha) and *post-rainy* (2.89 m ha) seasons [4]. Nearly 1.5 m ha of cropped area is also under use for forage sorghum, which is cultivated during the summer season. More than 90% of the sorghum cropped area in the country is grown under rainfed conditions. Rainy season sorghum is cultivated under both sole (40%) and intercrop (along with pulses and oilseeds) (60%) cropping systems. However, the *post-rainy* sorghum is preferred to cultivate as a sole crop under residual soil moisture conditions.

Sorghum is cultivated for diverse uses, such as food and feed purposes. The forage of the crop is highly nutritious for livestock animals. The crop also has a significant capacity for ethanol production and has been identified as a potential biofuel crop. Sorghum grains are the richest sources of Fe and Zn minerals, apart from starch and protein [5,6]. Since the late 1990s, there has been a remarkable shift in the sorghum cropped area from the monsoon to the *post-rainy* season. The area proportions between monsoon (62%) and *post-rainy* seasons (38%) in the total sorghum cropped area during 1960s has been altered to 39% (monsoon) and 61% (*post-rainy*) by 2020–2021 [4]. The rain that occurs during the rainy season exactly coincides with the time of the rainy season sorghum harvest, resulting in poor quality for the grains due to grain mold attacks and fetching lower market prices. In spite of significant crop improvement exertions by both the public and private sectors [7], the rainy season cropped area has been eroded in the country due to low profitability in its cultivation. The majority of the rainy season's produce is diverted for industrial usage (mainly poultry) rather than human consumption [8,9]. Relatively, the average productivity levels are higher for the monsoon season sorghum because of good access to modern cultivars, including hybrids. The mean productivity levels are lower in the case of the *post-rainy* crops due to the non-availability of improved cultivars and moisture stress conditions. However, the quality of the grain is superior in the *post-rainy* season compared with that of the monsoon season. Grain molds and shoot fly attacks during the rainy season often deteriorate the quality of monsoon production. A major chunk of the *post-rainy* season produce is diverted for human consumption and fetches higher market prices (nearly double) than rainy season grain. In both seasons, stover (straw) forms an important source of crop income as well as animal feed for their livestock. The leading states for growing *post-rainy* season sorghum in India are Maharashtra, Karnataka, Andhra Pradesh, Gujarat and Telangana. It is an important source of food, fodder and livelihood for the sorghum growers in the niche areas located in these states.

Historically, sorghum is a climate resilient crop which developed its drought tolerance traits to withstand and respond to adverse climate conditions. It is a perfect crop for the semi-arid tropics (SAT), which is a permanent home for the poorest of the poor people. Sorghum can thrive well under excessive temperatures, salt and waterlogging situations. It is well-established that sorghum is a good potential crop for promoting household incomes as well as lifting the poor out of poverty [10]. Under the perils of climate change and variability (CCV), the plausible impacts on crop productivity levels across the world, especially in the tropics, are going to be very high. Increasing temperatures coupled with significant deviations in the annual rainfall distribution may exacerbate substantial negative effects in SAT regions [11,12]. *Post-rainy* sorghum is likely to reduce its productivity per ha up to 7% by 2020, up to 11% by 2050 and up to 32% by 2080 due to anticipated climate change projections. The probable impacts will be severe and may vary its intensity across the *post-rainy* sorghum-cultivating agro-ecologies of India [13]. The introduction of climate-smart cultivars and an improved package of practices may compensate for the plausible impacts partially. However, significant crop productivity loss was noticed after a 2 °C rise in temperature and even after providing twice the quantity of rainfall across the major cultivating regions in India [13].

With this background, it is highly important to deeply understand the potential impacts of the future climate on *post-rainy* sorghum crop performance in India. Researchers have attempted to comprehend this with either one or two future climate change scenarios

previously [13]. There is scanty information or evidence on plausible climate change impacts on the crop using a whole range (multi-model) of climate change projections. It would be highly interesting to see and understand the entire gamut of those plausible impacts under diverse sorghum agro-ecological conditions in India. This will immensely help us to define and develop location-specific and tailor-made climate change mitigation strategies and management practices well in advance. The present research paper makes robust and systematic efforts to quantify the plausible future climate change impacts on *post-rainy* sorghum performance in India using both crop simulation and multi-model climate scenarios. This exercise will showcase the potential climate change impacts on *post-rainy* sorghum crops across the studied states in India. The findings in this paper will help scientists, agronomists and policymakers in designing suitable climate adaptation strategies and policies for crop improvement. The outcome of this paper will help in protecting the livelihoods of millions of rainfed farmers who are directly or indirectly dependent on *post-rainy* sorghum cultivation in India and their associated livestock population. The lessons learned in India could be scaled up to other similar regions around the world.

2. Materials and Methods

2.1. Climate, Soil and Crop Management Data

The gridded daily data of the rainfall (0.25° latitude × 0.25° longitude) and both the maximum and minimum surface temperatures (0.5° latitude × 0.5° longitude) were obtained from the India Meteorological Department (IMD) for 25 years (1981–2005). Incoming solar radiation (Q) was computed using the Bristow and Campbell (1984) model. The model developed a relationship between the fraction of daily total transmission and the daily time scale air temperature extremes range (D):

$$Q = Q_0\, a(1 - \exp(-bD^c)) \quad (1)$$

The empirical coefficients (a, b and c) for the specific location were determined from the solar radiation data measured for that location. The diurnal range of the surface air temperature (D) was calculated as

$$D = T_{max} - \frac{T_{min}(j) + T_{min}(J+1)}{2} \quad (2)$$

where T_{max} is the daily maximum temperature (°C), T_{min} (j) is the minimum temperature (°C) of the day and T_{min} (j + 1) is the minimum temperature recorded on the next day. The model included an adjustment for the measured D on rainy days, as cloud cover can be another manifestation of rainfall.

Bio-physical crop simulation models require profile-wise soil information, and in this study, we used soil data from SoilGrids1km developed by the International Soil Reference and Information Centre (ISRIC) in collaboration with several international agencies [14]. However, as the rainfall data were available only at a 0.25 × 0.25 degree spatial resolution, we restricted the crop simulations to 0.25 × 0.25 degrees, as simulating 1-km soil grids is computationally every expensive. Soil profiles were overlayed on rainfall grids, and the soil profile that had the maximum area under the rainfall grid was selected. SoilGrids1km offers both the physical and chemical properties of soil profiles at six depth intervals: 0–5, 5–15, 15–30, 30–60, 60–100 and 100–200 cm. The soil properties include sand, silt and clay fractions (%), bulk density (kg m^{-3}), soil organic carbon (g kg^{-1}), pH, cation exchange capacity (cmol kg^{-1}) and coarse fragments (%). To simulate the growth, development and yield of major *post-rainy* season sorghum growing environments in India, we used the Spatial Production Allocation Model (SPAM) of the International Food Policy Research Institute (IFPRI) to identify plausible sorghum crop distribution (IFPRI, 2019) maps in India.

The general recommended package of practices for *post-rainy* season sorghum was presumed to mimic on-farm crop management practices [15–18]. General information on the crop management aspects across *post-rainy* season sorghum growing regions were

collected from a literature review. Critical analysis on the information compiled revealed that the crop was usually sown within a short planting window between the end of September and the first half of October. The actual planting date during the sowing window was set based on the criteria of 25 mm of rainfall received in 10 days using a crop simulation model that would facilitate successful emergence and early crop establishment. The cultivar used in this study was M 35-1, and the validated and calibrated DSSAT crop coefficients for M 35-1 were taken from previous studies [19,20] based on long-term All India Coordinated Research Project on Sorghum (AICRPS) trials. In this study, we initialized the simulation start on the first day of August, with sowing performed when the sowing criteria were met. The M 35-1 genotype was sown with a plant density of 12 plants per m^2 along with nitrogen @ 20 kg/ha applied as a basal dose. Furthermore, 30 kg ha^{-1} was applied 30 days after sowing. The simulation was run at a 0.25° × 0.25° resolution scale.

2.2. Climate Scenarios and Bias Correction Technique

The Earth System Models (ESMs) and the General Circulation Models (GSMs) are the most cutting-edge tools currently available to model changes in the global climate to increase in the planet's radiative forcing at large spatial and temporal scales. The impact assessment user community of such projections often needs higher spatial resolutions to understand the impacts of climate change seen at regional and local scales. To accommodate such finer information, the global climate model projections were downscaled through dynamical and statistical approaches, as the GCMs' simulation precisions were poor due to a coarse spatial resolution [11,21]. The Earth Exchange Global Daily Downscaled Projections (NEX-GDDP) datasets of the National Aeronautics and Space Administration (NASA) at high spatial (~25 km × 25 km) and temporal (daily) resolutions were composed of bias-corrected and statistically downscaled climate scenarios derived from 20 GCMs (Table 1) of the coupled model inter-comparison project phase 5 (CMIP5) across two Representative Concentration Pathways (RCPs)—4.5 (mid-range emissions) and 8.5 (high-end emissions)—used in this study. The downscaled climate change projections included the rainfall and maximum and minimum temperatures for the period from 1950 to 2005 (retrospective run) and from 2006 to 2099 (prospective run). The Bias-Corrected Spatial Disaggregation (BCSD) method was used to generate these datasets [22,23]. The NEX-GDDP datasets have been cited as the most promising high-resolution climate change scenarios for carrying out impact studies on the aspects of climate change from the local to regional scales [24]. In the present study, we used the multi-model mean (MMM) approach to evaluate the performance of the NEX-GDDP data (temperature and precipitation) over the historical climate of India with the India Meteorological Department (IMD) (Pune, India) developing daily high-resolution 0.25° × 0.25° gridded rainfall and 0.5° × 0.5° gridded temperature data. The advantage of using the multi-model mean (MMM) was that it performed better than the individual model and averaged out the internal variability when compared with the observations. The current study explores the projected changes in the *post-rainy* season simulated trajectories of sorghum yields over eight states in India in the near future (2040–2069) and far future (2070–2099) with reference to the baseline period (1981–2015). The projected changes in precipitation and temperature were analyzed using these high-resolution datasets.

Table 1. List of GCMs in the NEX-GDDP dataset used in the study.

No.	Organisation	Model Name	Country	Grid Resolution
1	Commonwealth Scientific and Industrial Research Organization (CSIRO) and Bureau of Meteorology (BOM) in Australia	ACCESS1.0	Australia	144 × 192
2	Beijing Climate Center, China Meteorological Administration	BCC-CSM1.1	China	64 ×128
3	Beijing Normal University	BNU-ESM	China	64 ×128
4	Canadian Centre for Climate Modelling and Analysis	CanESM2	Canada	64 ×128
5	National Center for Atmospheric Research	CCSM4	USA	192 × 288
6	National Science Foundation, Department of Energy, NCAR	CESM1-BGC	USA	192 × 288
7	Centre National de Recherches Meteorologiques, Centre Europeen de Recherche et Formation Avancees en Calcul Scientifique	CNRM-CM5	France	128 × 256
8	Commonwealth Scientific and Industrial Research Organization in collaboration with the Queensland Climate Change Centre of Excellence	CSIRO-Mk3.6.0	Australia	96 × 192
9	NOAA Geophysical Fluid Dynamics Laboratory	GFDL-ESM2G GFDL-ESM2M	USA USA	90 × 144 90 × 144
10	Institute for Numerical Mathematics	INM-CM4	Russia	120 × 180
11	Institut Pierre-Simon Laplace	IPSL-CM5A-LR IPSL-CM5A-MR	France France	96 × 96 143 × 144
12	Japan Agency for Marine-Earth Science and Technology, Atmosphere and Ocean Research Institute (The University of Tokyo), and National Institute for Environmental Studies	MIROC-ESM MIROC-ESM-CHEM	Japan Japan	64 × 128 64 × 128
13	Atmosphere and Ocean Research Institute (The University of Tokyo), National Institute for Environmental Studies and Japan Agency for Marine-Earth Science and Technology	MIROC5	Japan	128 × 256
14	Max Planck Institute for Meteorology	MPI-ESM-LR MPI-ESM-MR	Germany Germany	96 × 192 96 × 192
15	Meteorological Research Institute	MRI-CGCM3	Japan	160 × 320
16	Norwegian Climate Centre	NorESM1-M	Norway	96 × 144

2.3. Crop Model Description and Yield Simulations

Crop Environmental Recourse Synthesis (CERES) sorghum modeling under Decision Support System for Agro-Technology Transfer (DSSAT) Version 4.7 [25] is a process-based comprehensive model to simulate the crop growth, development and final grain yield of sorghum. Using a daily time step routine, the model simulates growth and development to the maturity stage based on the complex physiological processes describing crop responses to weather conditions, soil and crop management practices. The cultivar-specific genetic coefficients specify the phenological development and growth based on the thermal time and photo-period conditions defined in the model. The model computes the net photosynthesis based on the light intercepted, and photosynthate is partitioned to different parts of the plant on a given day while constrained by temperature, water deficit, and nutrient stress factors [26,27]. This model can be effectively used for understanding the impacts of climate change on *post-rainy* sorghum growth and yield across dry region tracts of India.

2.4. Crop Model Evaluation Protocols

For evaluation of the simulation's outputs, we used the mean sorghum yield data product reported at the district level during the *post-rainy* season across the study states in India. The simulated sorghum yield at a 0.25° × 0.25° spatial resolution was subsequently aggregated to the district administrative boundaries. Model performance in reproducing the observed historical yields at the district level was evaluated by calculating the absolute and normalized mean root square error, coefficient of determination (R^2) and the Wilmot d index [28]. The ability of the CERES sorghum model to reproduce historical yields was determined by the values of the RMSE and d index. A good agreement between the observed and simulated yields was represented by a lower root mean square error (*RMSE*) and a d value close to one. The relative difference between the observed and simulated yields was represented by the normalized *RMSE* (%). In the present study, based on [29], the performance of the simulation model was categorized into four categories: excellent, good, fair and poor, depending on the normalized *RMSE* (NRMSE) values of <10%, 10–20%, 20–30% and >30%, respectively. The equations for elevating the model performance were as follows:

$$RMSE = \left[n - 1 \sum_{i=1}^{n} (P_i - O_i)^2\right]^{0.5} \quad (3)$$

where P_i and O_i are the simulated and observed values, respectively, and n is the number of observations:

$$normalised\ RMSE\ (\%) = \left(\frac{absolute\ RMSE}{\overline{O}}\right) \times 100 \quad (4)$$

where O is the average observed yield value [29], and

$$d - index = 1 - \left[\frac{\sum_{i=1}^{n} (P_i - O_i)^2}{\sum_{i=1}^{n} \left[P_i' + O_i'\right]^2}\right] \quad (5)$$

where n is the number of observations, P_i is the simulated yield, O_i is the observed yields at the district level and P_i' and O_i' are calculated as $P_i' = P_i - M$ and $O_i' = O_i - M$ (where M is the mean observed yields) [30].

3. Results

3.1. Evaluation of the CMIP5 Multi-Climate Model Mean (MMM)

To understand the spatial distribution of southwest (SW) and northeast (NE) monsoon rainfall, which represent the dominant climatic features, we calculated the mean seasonal rainfall totals of the two seasons for both IMD (1981–2005) and the NEX-GDDP baseline period. The west coast of India and parts of northeast India receive high rainfall amounts (1700–3000 mm). Central India receives about 1000 mm, while southern India receives rainfall ranging from 500 to 800 mm. Figure 1 clearly demonstrates that the multi-model mean (MMM) for the historical NEX-GDDP June through September (JJAS) precipitation mimicked the spatial distribution of IMD rainfall across India. However, the MMM rainfall tended to underestimate the rainfall totals in the western ghats, where average SW rainfall totals varied from 2000 mm to 4300 mm. The low-pressure system and tropical storms originating in the Bay of Bengal or the Arabian Sea and traveling toward the Indian land-mass contributed most of the SW monsoon rainfall over India. Southeast India, particularly Tamil Nadu and the bordering regions of other states (Andhra Pradesh, Karnataka and Kerala), received substantial rainfall amounts during the NE season (OND). The MMM of the NEX-GDDP models reasonably simulated the seasonal rainfall totals for both the SW and NE monsoon seasons.

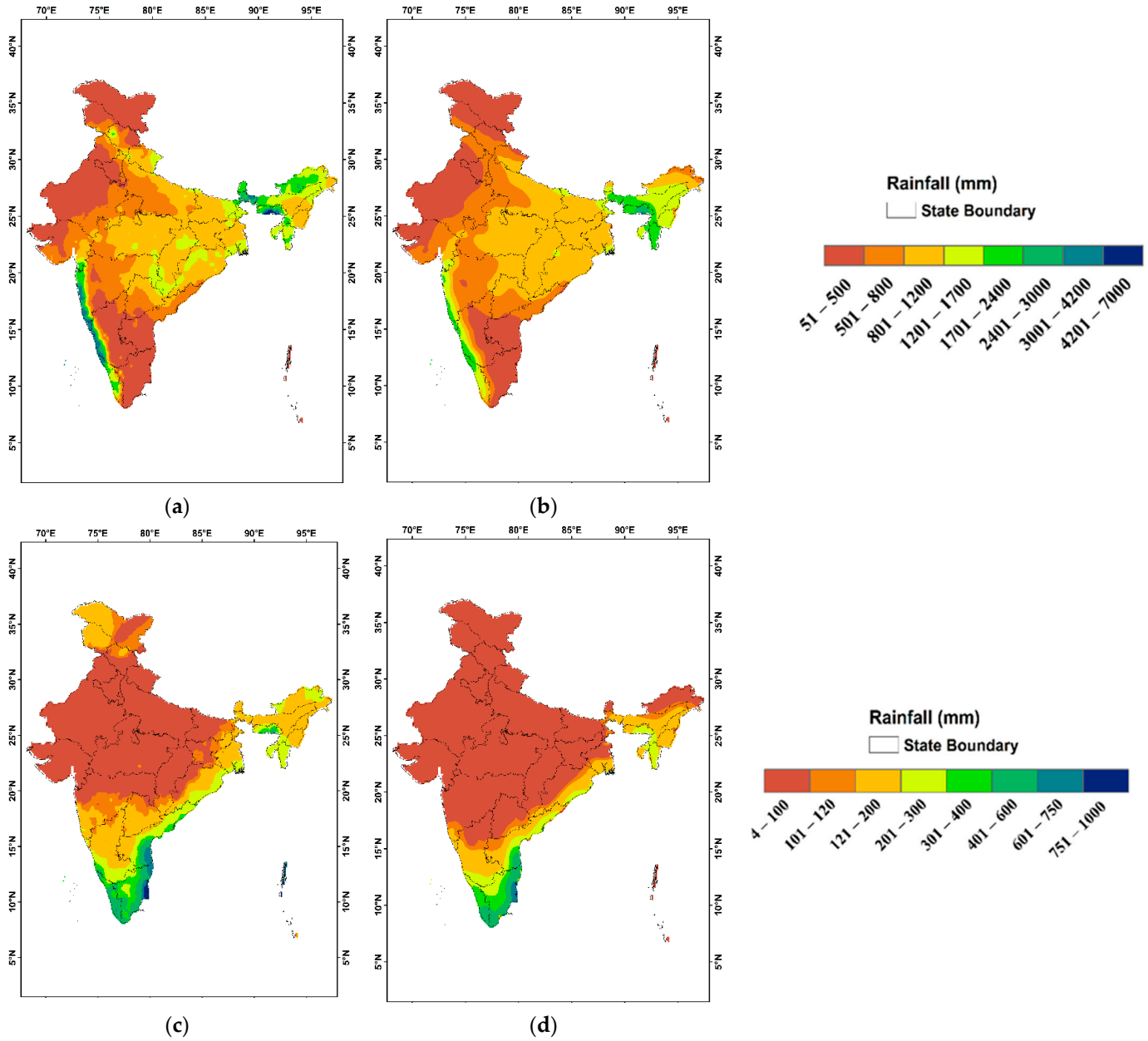

Figure 1. Comparison of NEX MMM and IMD spatial distribution of the mean SW (JJAS) and NW (OND) rainfall totals over India from 1981 to 2005: (**a**) IMD (JJAS); (**b**) NEX_MMM (JJAS); (**c**) IMD (OND); and (**d**) NEX_MMM (OND).

The NE monsoon rainfall is the primary source of water for crops grown under rained conditions. The interannual variability in NE monsoon rainfall over India (area averaged) is characterized by excesses and deficits in the rainfall totals, and agricultural productivity during the *post-rainy* season is significantly influenced by the NE monsoon rainfall totals. The climatology of NE monsoon rainfall as simulated by the multi-model mean (MMM) of 20 NEX-GDDP models for the baseline period of 1981–2005 is shown in Figure 1. The rainfall over the east coastal belt and the state of Tamil Nadu simulated by the MMM was in good agreement with the IMD climatology. The tropical storms and low-pressure systems over the Bay of Bengal during the OND months were associated with the rainfall received during the NE monsoon over southern India. Most of the region received substantial rainfall due to the formation of these storms. The MMM simulated the NE monsoon reasonably well and provided a realistic representation of the mean NE monsoon pattern.

To assess the ability of the MMM to reproduce SW and NE monsoon rainy days over India, we compared the model's simulated mean rainy days with the observed mean rainy days (Figure 2). The MMM simulated rainfall indicated a daily rainfall amount of 0.1 mm during dry periods. The rainfall series were first subjected to reducing the number of rainy days by using a cut-off (<1 mm) threshold for the rainfall. In both seasons (Figure 2), the MMM simulated rainy days were relatively higher. However, during the NE monsoon season, rainy days represented a similar spatial pattern to that observed in the IMD data.

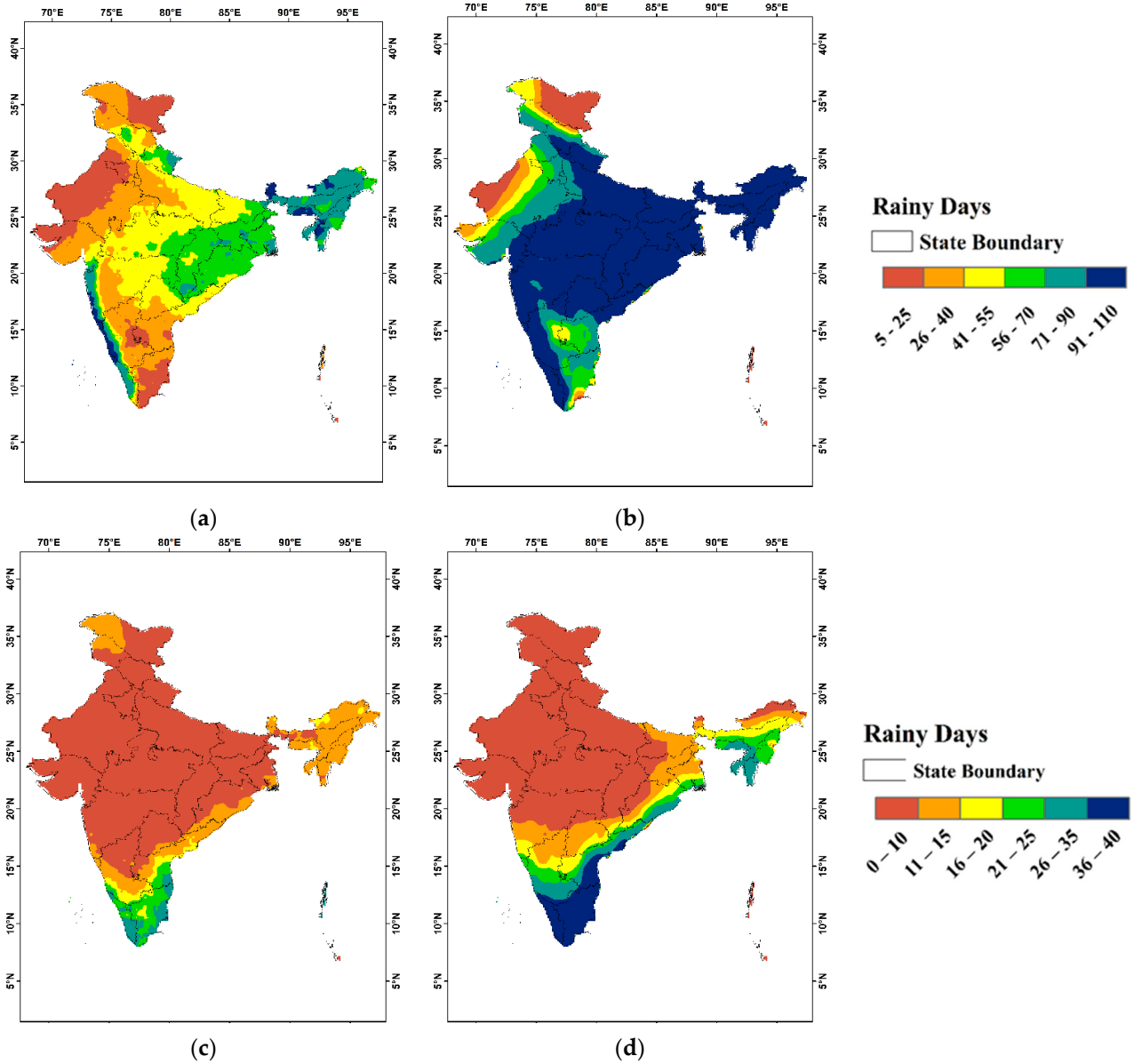

Figure 2. Comparison of NEX MAM and IMD spatial distributions of the mean SW (JJAS) and NW (OND) rainy days over India from 1981 to 2005: (**a**) IMD (JJAS); (**b**) NEX_MMM (JJAS); (**c**) IMD (OND); and (**d**) NEX_MMM (OND).

The spatial distributions of the climatological mean maximum and minimum temperatures over India are shown in Figures 3 and 4. The MMM of the NEX-GDDP represented good agreement with the mean spatial distributions of the maximum and minimum temperatures over India during the SW monsoon period. The MMM tended to overestimate the maximum and minimum temperatures during the JJAS period over the northwest parts of India, particularly over parts of the Gujarat and Rajasthan states. The MMM simulations

during the NE monsoon periods were well-represented spatially over the Indian subcontinent. The MMM captured the spatial distributions of both the maximum and minimum temperatures in the southern and central parts of India, where *post-rainy* season sorghum is predominantly cultivated. It is important to evaluate the performance of the MMM datasets in reproducing the monthly rainfall totals (annual cycle) over India, where both SW and NE monsoons display dominant climatic features.

The annual cycle of rainfall is shown in Figure 5 using a Hovmoller diagram. The figure shows the climatological annual cycle of rainfall over the Indian subcontinent for the IMD and MMM of the NEX-GDDP data. The IMD rainfall showed a clear temporal evolution in the monthly rainfall, with the intense rainfall regions located between 20 and 25° N, and the MMM of the NEX-GDDP reproduced the observed pattern with some difference in rainfall magnitude. Overall, the MMM datasets showed good agreement against the IMD rainfall.

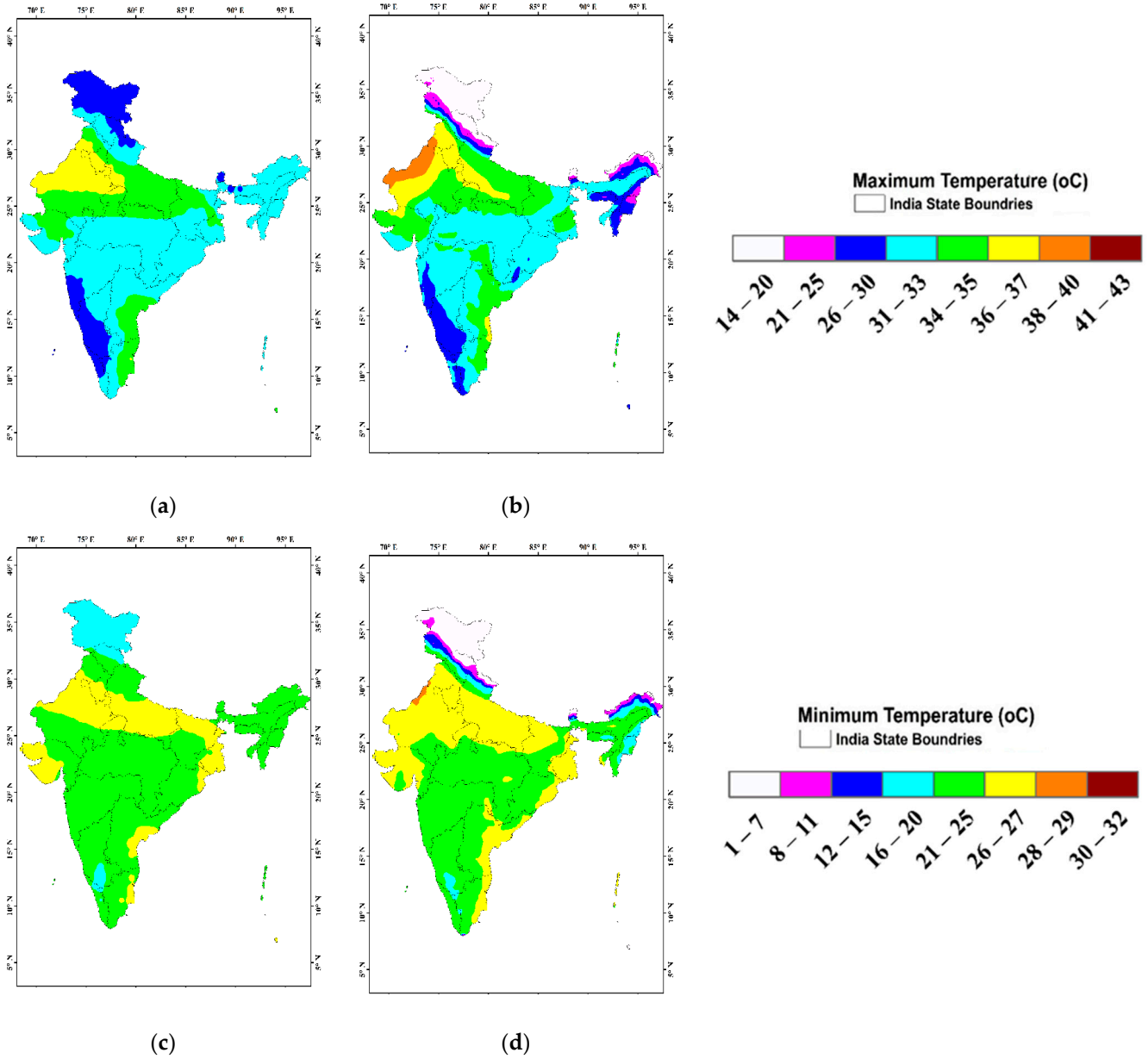

Figure 3. Comparison of NEX MAM and IMD spatial distributions of mean SW (JJAS) maximum and minimum temperatures over India from 1981 to 2005: (**a**) IMD (JJAS); (**b**) NEX_MMM; (**c**) IMD (JJAS); and (**d**) NEX_MMM (JJAS).

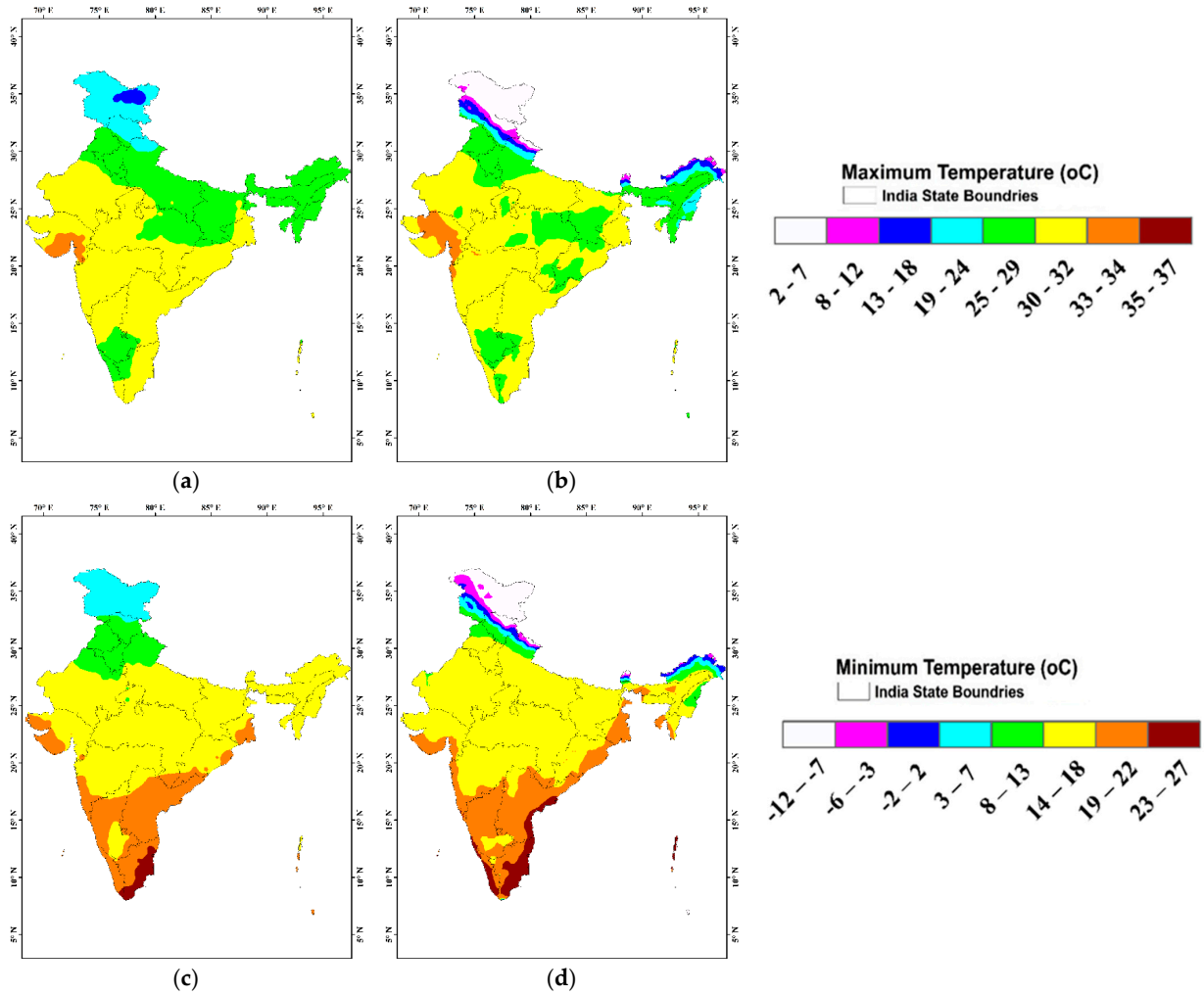

Figure 4. Comparison of NEX MAM and IMD spatial distributions of mean NE (OND) maximum and minimum temperatures over India from 1981 to 2005: (**a**) IMD (OND); (**b**) NEX_MMM (OND); (**c**) IMD (OND); and (**d**) NEX_MMM (OND).

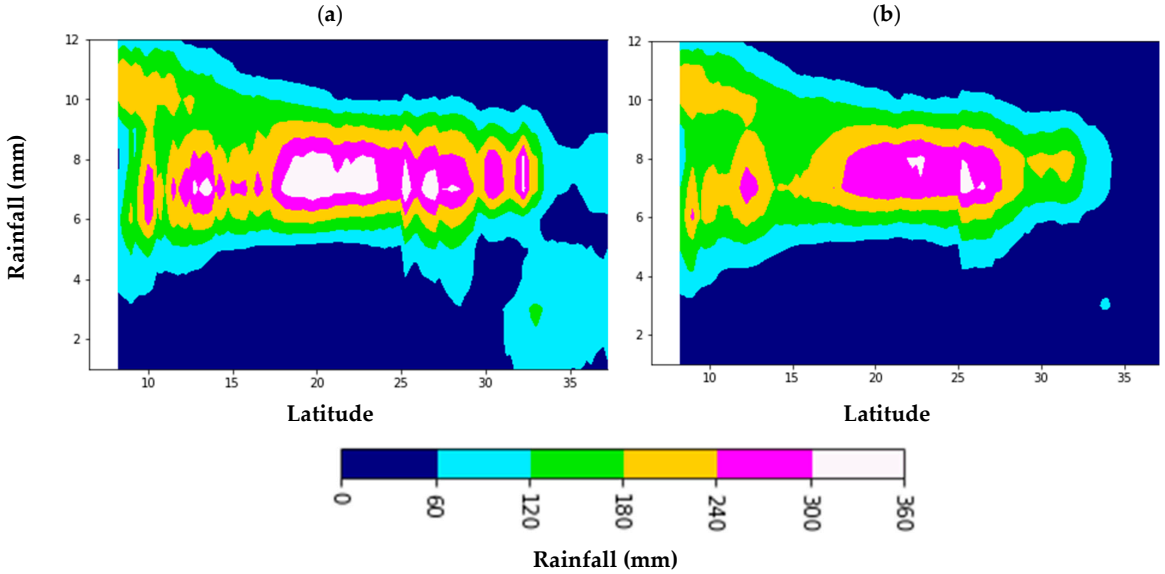

Figure 5. Hovmoller diagram displaying annual cycle of monthly rainfall climatology (mm/month) during 1981–2005 over the Indian subcontinent: (**a**) IMD rainfall and (**b**) MMM of NEX-GDDP.

3.2. Climate Change Scenarios

Global climate change is a long-term phenomenon, with a gradual increase in global temperatures due to enhanced anthropogenic greenhouse gas emissions. Such changes will lead to widespread impacts on natural systems. In this context, we discuss here the projected changes in precipitation and temperatures during the SW and NE monsoon seasons over India. For the SW monsoon period, rainfall amounts are increasing over India. However, the increase in rainfall amounts varies in magnitude both spatially and temporally. RCP 4.5 and RCP 8.5 near future projections indicate that the rainfall amounts are increasing over central India from 90 to 150 mm/season, while in the southwest regions (western ghats) and northeast parts of India, rainfall amounts are increasing from 250 to 450 mm/season. Rainfall amounts are further increasing in the far future in both RCP 4.5 and 8.5, with much of the increase noticed over the central, southwest and northeastern parts of India as displayed in Figure 6. The NE monsoon rainfall amounts are predominantly received over the southern peninsular India (SPI) states, and the MMMs of the NEX-GDDP simulations indicate that rainfall amounts are increasing during the NE monsoon period from 60 to 150 mm/season during the near future for both the RCPs (4.5 and 8.5). By the end of the 21st century, the NE monsoon rainfall amounts are projected to increase from 150 to 300 mm/season over the SPI states.

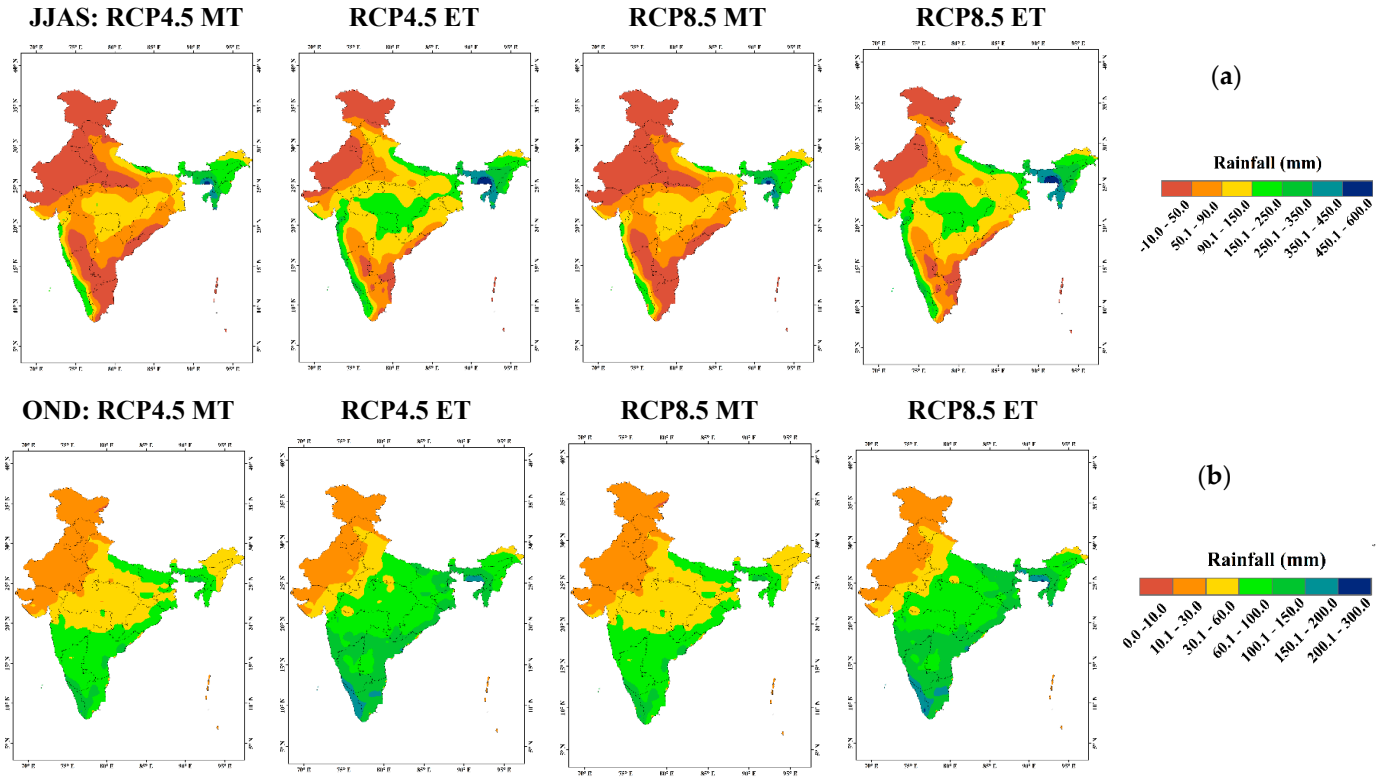

Figure 6. Projected mean changes in seasonal rainfall amounts over India during two time periods (middle and end of century): (**a**) SW and (**b**) NE monsoons.

The past and future trends in the mean maximum, minimum temperatures and precipitation are depicted in Figure 7. The IMD mean's Simple Daily Intensity Index (SDII) exhibited a marginal increasing trend during both the SW and NW monsoon seasons with high interannual variability. The MMMs of the NEX-GDDP baseline datasets presented very low inter-annual variability during the SW monsoon period. However, during the NE monsoon period, the interannual variability was relatively higher compared with the IMD SW monsoon period, and the year-to-year variability of the MMM-generated SDII during the NW season was still underestimated compared with the IMD SDII. The long-term time series of IMD rainfall (1951–2005) indicated a marginal increase in rainfall amounts during

the SW and NE monsoon seasons of about 0.04 and 0.07 mm/decade, respectively. Baseline simulations of the MMM of the NEX-GDDP exhibited an increase in rainfall of about 0.03 and 0.04 mm/decade during the SW and NE monsoon periods, respectively. Projected changes in the mean SW and NE monsoon rainfall during the near future (2040–2069) and far future (2071–2099) with respect to the baseline (1976–2005) showed an unswerving increase in the mean rainfall amounts under both RCPs (4.5 and 8.5). The future projections of the MMM rainfall indicated a likely increase in the mean rainfall amounts during the SW monsoon period across India (approximately 2% under RCP 4.5 in the near future and 6% by the far future). The RCP 8.5 projections showed a consistent increase in the mean SW monsoon rainfall over India (around 6% by the near future and 10% by the far future). The projected changes during the NE monsoon period over India indicate a more pronounced increase in rainfall amounts under two emission scenarios: under RCP 4.5 rainfall amounts, which are expected to increase by around 5% during the near future and 20% by the far future, and under the RCP 8.5 emission scenario, where the rainfall amounts are likely to increase up to 8% in the near future and 23% in the far future.

The mean maximum and minimum temperatures were gradually increasing in the future scenarios (RCP 4.5 and 8.5) across India. However, the trend was more prominent under RCP 8.5. This can be noticed through the trajectories of the future projected temperatures, which display a substantial increase under the RCP 8.5 scenario compared with RCP 4.5. The projected changes in air temperatures during the near future and far future under both RCPs relative to the NEX baseline period (1976–2005) indicate a consistent increase in the mean maximum temperature, with RCP 4.5 suggesting a maximum increase of 1.4 °C in the near future to 1.7 °C in the far future over the Indian subcontinent during the SW monsoon period. Meanwhile, during the NE monsoon period, the projected changes in the mean maximum temperature are expected to increase up to 1.6 °C by the near future and 1.8 °C by the far future. The RCP 8.5 scenario projected an increase in the mean maximum temperature during the SW monsoon period of 2.0 °C during the near future and 3.4 °C for the far future. The mean maximum temperature during the NE monsoon period is projected to increase by 2.1 °C and 3.5 °C for the near and far future, respectively. During the SW monsoon period, the mean minimum temperature for the near and far future showed an increase of 1.6 °C and 2.0 °C, respectively, under the RCP 4.5 scenario. Meanwhile, during the NE monsoon period, the increase in the mean minimum temperature was 1.7 °C and 2.0 °C for the near and far future, respectively. Under the RCP 8.5 scenario, the increase in the mean minimum temperature was more pronounced, being 2.3 °C and 3.7 °C for the SW monsoon period for the near and far future, respectively, whereas for the NE monsoon period, the increase was about 2.5 °C and 4.1 °C for the near and far future, respectively. It was noticed that during both of the periods (near and far future), the projected mean minimum temperature was higher than the mean day temperatures.

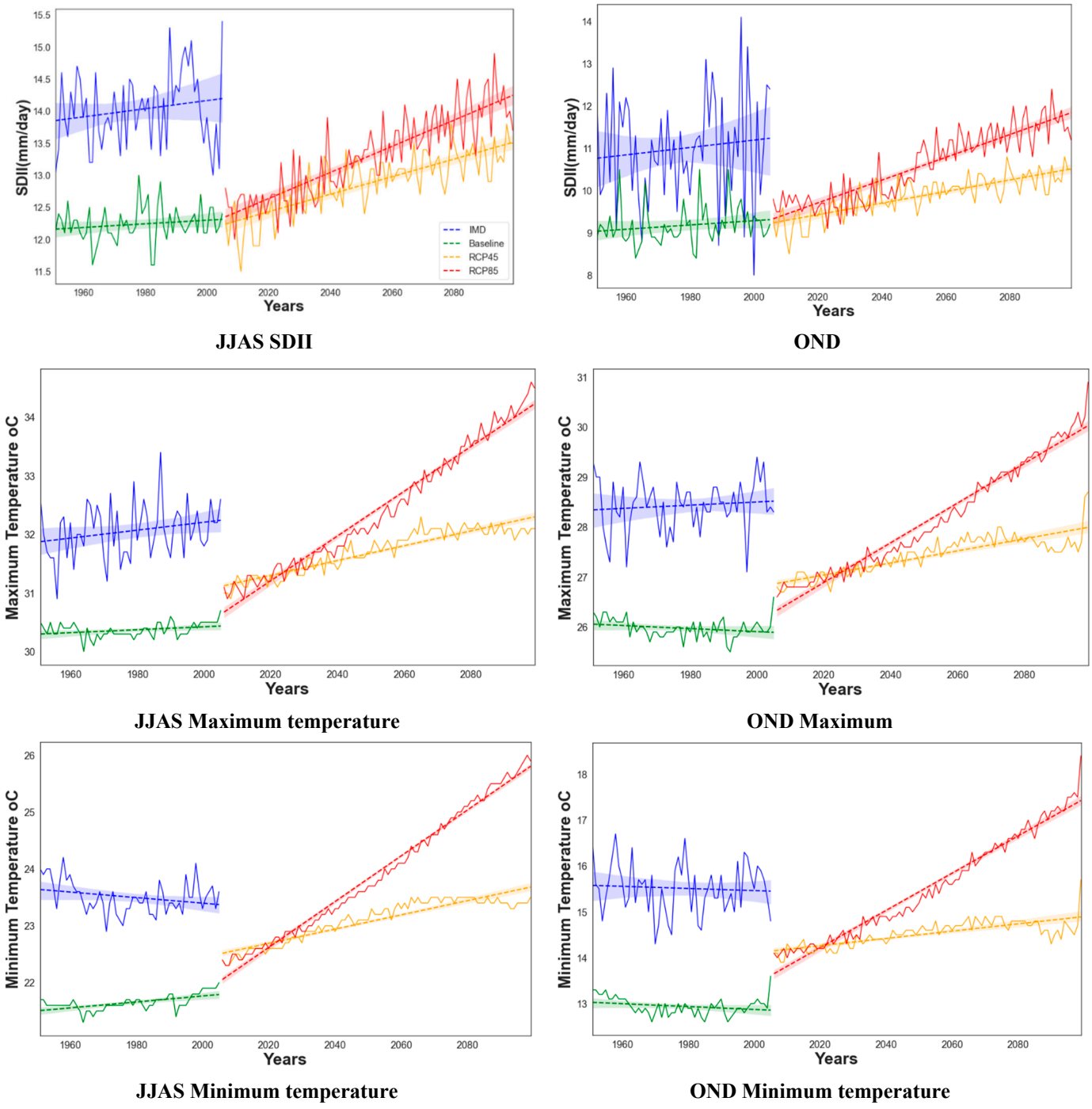

Figure 7. Time series of interannual variability of simple daily intensity index of rainfall during SW (JJAS) and NW (OND) monsoon seasons over India (top), as well as the maximum temperature (middle) and minimum temperature (bottom), IMD (blue), baseline (green), RCP34 (orange) and RCP85 (red).

3.3. Evaluation of the Simulated Yields under the Historical Period

The CERES-sorghum model was configured to be run in a gridded mode at the IMD spatial resolution (approximately 25 km × 25 km). The input requirements of the CERES-sorghum model for each grid were developed spatially at a 25-km resolution. The performance of the CERES-sorghum model, which was driven by the observed climate data for the *post-rainy* season sorghum crop during 1981–2015, was evaluated. The comparison of the observed and simulated sorghum yields for the 64 districts that fell under 8 major *post-*

rainy season sorghum growing states are displayed in Figure 8a,b. The simulated sorghum grain yields showed higher yields compared with the observed yields across the sorghum growing states. The higher simulated sorghum yields perhaps echoed the fact that the crop simulation model was well-fertilized, good crops were established, and it was free from biotic stress conditions. Consequently, similar assumptions at larger geospatial scales, such as districts and states, resulted in higher sorghum yields. The relatively higher interannual variability in the simulated sorghum yields was most likely due to the coarse spatial resolution of the observed climate information. The evaluation statistics for measuring the performance of the CERES-sorghum model for different environmental conditions are presented in Table 1. The coefficient of determination (R^2) between the simulated and the observed sorghum grain yields for the 8 states was 0.87 (n = 264, $p < 0.001$), and the root mean square error was 270 kg ha^{-1} (Table 2). The Wilmot d index was 0.82, and the evaluation statistics indicate that the CERES-sorghum crop model was in good agreement with the observed grain yields.

Table 2. Descriptive statistics displaying the capability of CERES-sorghum model in reproducing historic yields.

	Yields (Kg/ha)		Coefficient of Determination (R2)	RMSE	NRMSE	d Index
	OBS	SIM				
Andhra Pradesh	1305	1447	0.73	217.09	0.17	0.86
Chhattisgarh	892	988	0.72	271.00	0.20	0.88
Gujarat	1034	1144	0.73	270.00	0.14	0.88
Karnataka	898	967	0.48	261.00	0.14	0.86
Maharashtra	858	909	0.36	255.12	0.13	0.82
Madya Pradesh	1467	1597	0.75	300.17	0.13	0.85
Telangana State	881	1017	0.40	301.44	0.23	0.67
Tamil Nadu	1786	1993	0.53	280.48	0.11	0.84

The simulated values of the sorghum grain yields for the period from 1981 to 2015 were significantly correlated with the observed yield data. (For the RMSE, the lowest was observed at Andhra Pradesh (217), and the highest was observed at Telangana and Madhya Pradesh states (301).) The d value, a measure of the model's performance in reproducing historic yields, was also high, varying from 0.67 in Telangana state to 0.88 in Chhattisgarh and Gujarat. These results illustrate that the genetic coefficients of the M 35-1 sorghum cultivar and crop management practices arrayed in the model simulations were presumed to be accurate, and the CERES-sorghum model could be applied to assess the possible potential impacts of climate change on the growth and yields of sorghum crops during the *post-rainy* season. Figure 8b compares the simulated and measured sorghum yield values for the eight states. The 1:1 line plot illustrates that the spread of simulated yields is relatively higher compared with the observed sorghum grain yield values. The statistical indices used to evaluate the performance of the CERES-sorghum model showed good agreement between the observed and modeled yields. The simulated *post-rainy* sorghum yields demonstrated good agreement with the spatial reporting (Figure 9), with the Tamil Nadu state-reported highest sorghum grain yield values ranging from 1200 to 2500 kg ha^{-1} and the CERES-sorghum model simulated yields for the historical period varying from 900 to 3200 kg ha^{-1}. Similarly, parts of Maharashtra, Karnataka, Madhya Pradesh and Gujarat reported that lower yields were spatially captured in the IMD runs.

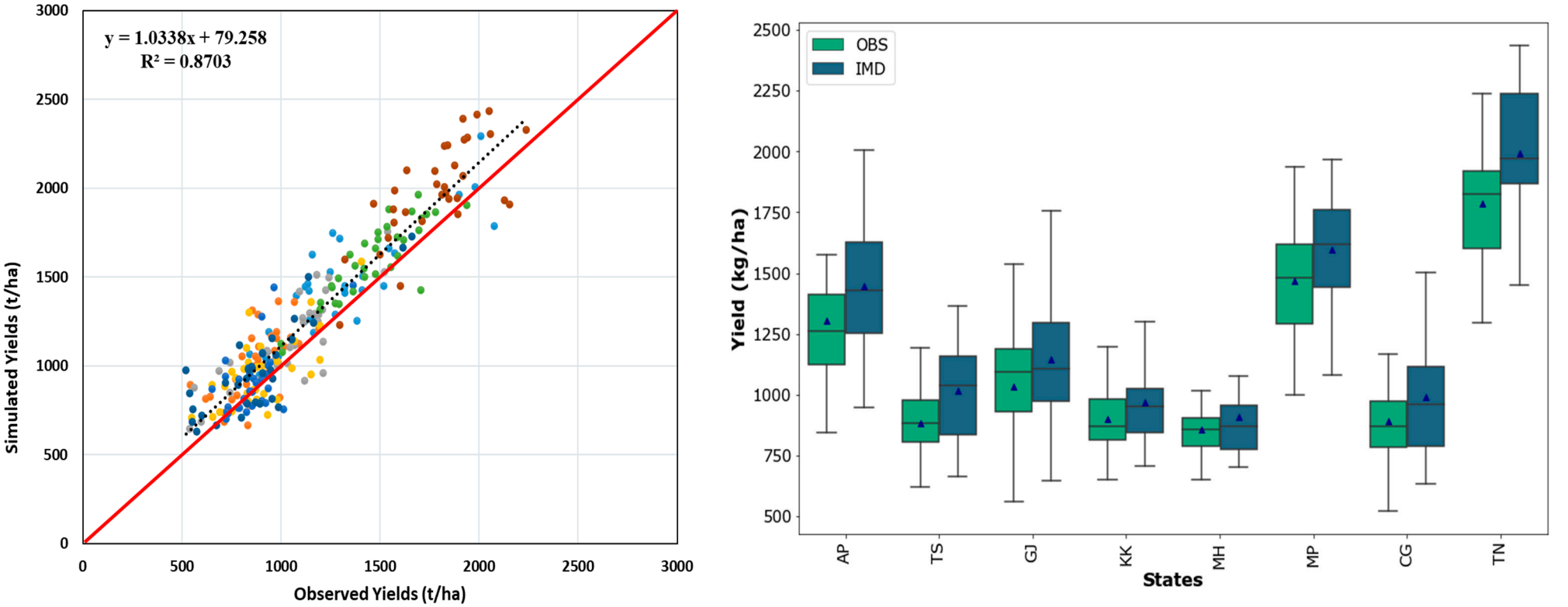

(**a**) (**b**)

Figure 8. (**a**) Relationship between observed and modeled *post-rainy* sorghum yields during 1981–2015. (**b**) Comparison of observed and modeled sorghum grain yields for the mean and variability across the study area. The eight states used in the study were as follows: AP = Andhra Pradesh; TS = Telangana state; GJ = Gujarat; KK = Karnataka; MH = Maharashtra; MP = Madhya Pradesh; CG = Chhattisgarh; and TN = Tamil Nadu.

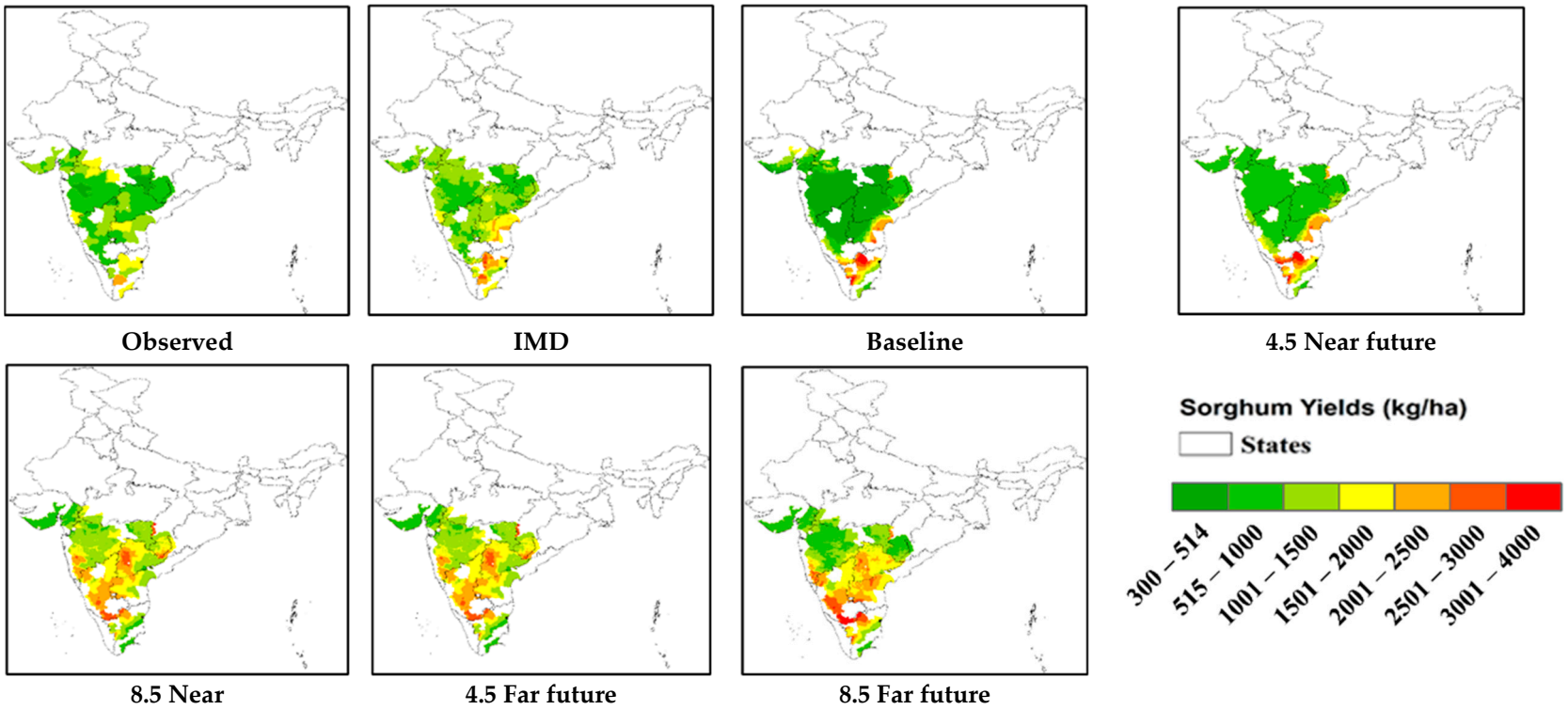

Figure 9. The maps express the spatial patterns of sorghum grain yields during the post-rainy season under each climatic condition. The images shows the reported yields, DSSAT-modeled historic yields using IMD-gridded climate data, simulated sorghum yields for the MMM baseline, RCP 4.5 near future, RCP 8.5 near future, RCP 4.5 far future and RCP 8.5 far future.

3.4. Impacts on Sorghum Yields

The CSM-CERES-sorghum simulation model attached with the seasonal analysis program in DSSAT V4.7 was used to understand the plausible impacts of climate change on sorghum growth and yields under two time periods (near future and far future) and two RCPs (4.5 and 8.5). Simulations were carried out for the baseline, 4.5 near future, 8.5 near future, 4.5 far future and 8.5 far future for each grid that fell within the sorghum growing regions of the selected states. Simulations were initiated on 1 August each year, and the soil profile at the start of the simulation was considered to be at the lower limit of soil water availability. The sowing window assumed was from 25 September to 15 October, and the simulated crop was sown on the day when the accumulated rainfall for 10 consecutive days was $\geq$25 mm.

The simulated sorghum grain yields for the MMM-baseline period across the selected states specified that the sorghum yields were lower compared with the observed and IMD-driven climate, except for Tamil Nadu. In response to climate change, the mean *post-rainy* sorghum yield values were found to be considerably increasing. Yield changes under the future climates (assuming unchanged management) for RCP 4.5 in the near future ranged from −3% (Gujarat) to 40% (Karnataka) on average. Under the climate change scenario, the spatial patterns of the sorghum yields displayed a similar pattern to the IMD-modeled yields (Figure 9). The simulated grain yields for RCP 4.5 in the near future varied from 0.8 t ha^{-1} (Maharashtra) to 2.0 t ha^{-1} (Tamil Nadu), aggregated at the state level. Under RCP 8.5 in the near future, the modeled sorghum grain yields varied from 0.82 t ha^{-1} in Maharashtra to 2.2 t ha^{-1} in Tamil Nadu, and the yields were marginally increasing (approximately 10%) under RCP 8.5 in the near future in Gujarat (6.3%), Tamil Nadu (8.8%) and Madhya Pradesh 11%). The highest increase was noticed in Telangana (59.3%), followed by Karnataka (45.6%), Andhra Pradesh (41.3%), Chhattisgarh (34.3%) and Maharashtra (25%). The projected changes in the far future under RCP 4.5 illustrate that the simulated sorghum yield values were further increasing up to 72% in Madhya Pradesh, and the lowest increase was noticed in Tamil Nadu (20.6%). The aggregated sorghum yields at the state level for RCP 4.5 in the far future varied from 1.0 t ha^{-1} in Maharashtra to 2.5 t ha^{-1} in Tamil Nadu. Similarly, under RCP 8.5 in the far future, the modeled sorghum yields showed that they were slightly higher than RCP 4.5 in the far future. The highest increase in sorghum yields was observed in Madhya Pradesh (89%), followed by Telangana (84%). A comparison of the yield variabilities across different climate scenarios and climate regimes (near future and far future) displayed high interannual variability in the modeled sorghum yields under the climate change scenarios. The modeled sorghum grain yields were relatively stable, with low CV in the reported yields followed by the IMD-simulated yield values. The baseline simulations exhibited high CV across all the states, with the highest interannual variability in the simulated yields noticed in RCP 8.5 in the far future. Both Tamil Nadu and Madhya Pradesh displayed high interannual variability in the simulated yields, followed by, in order, Chhattisgarh, Maharashtra, Karnataka, Andhra Pradesh, Telangana and Gujarat. Furthermore, the higher yields were spatially observed in the southern region of India covering Tamil Nadu, Karnataka, Andhra Pradesh and Telangana (Figure 10).

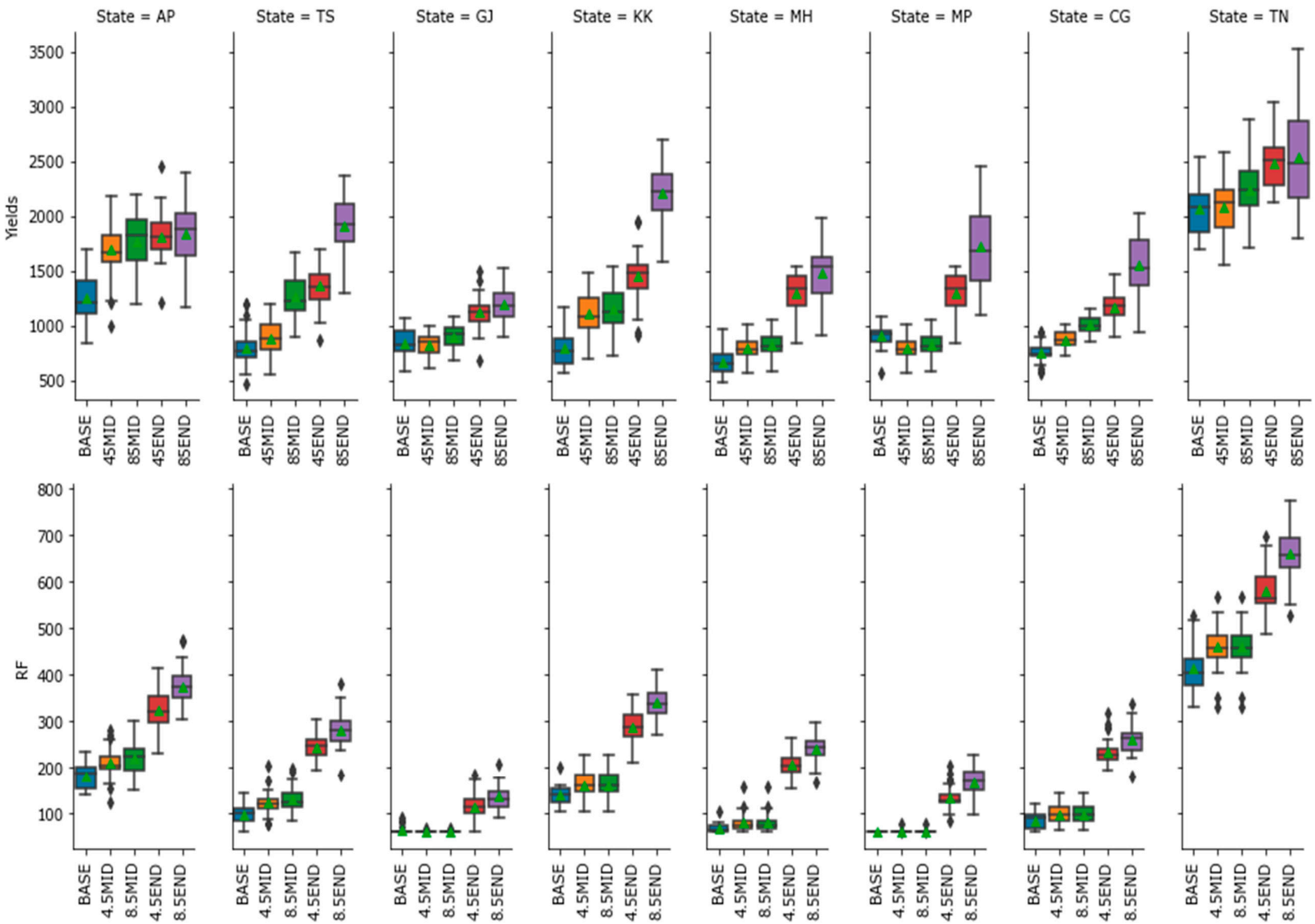

Figure 10. *Cont*.

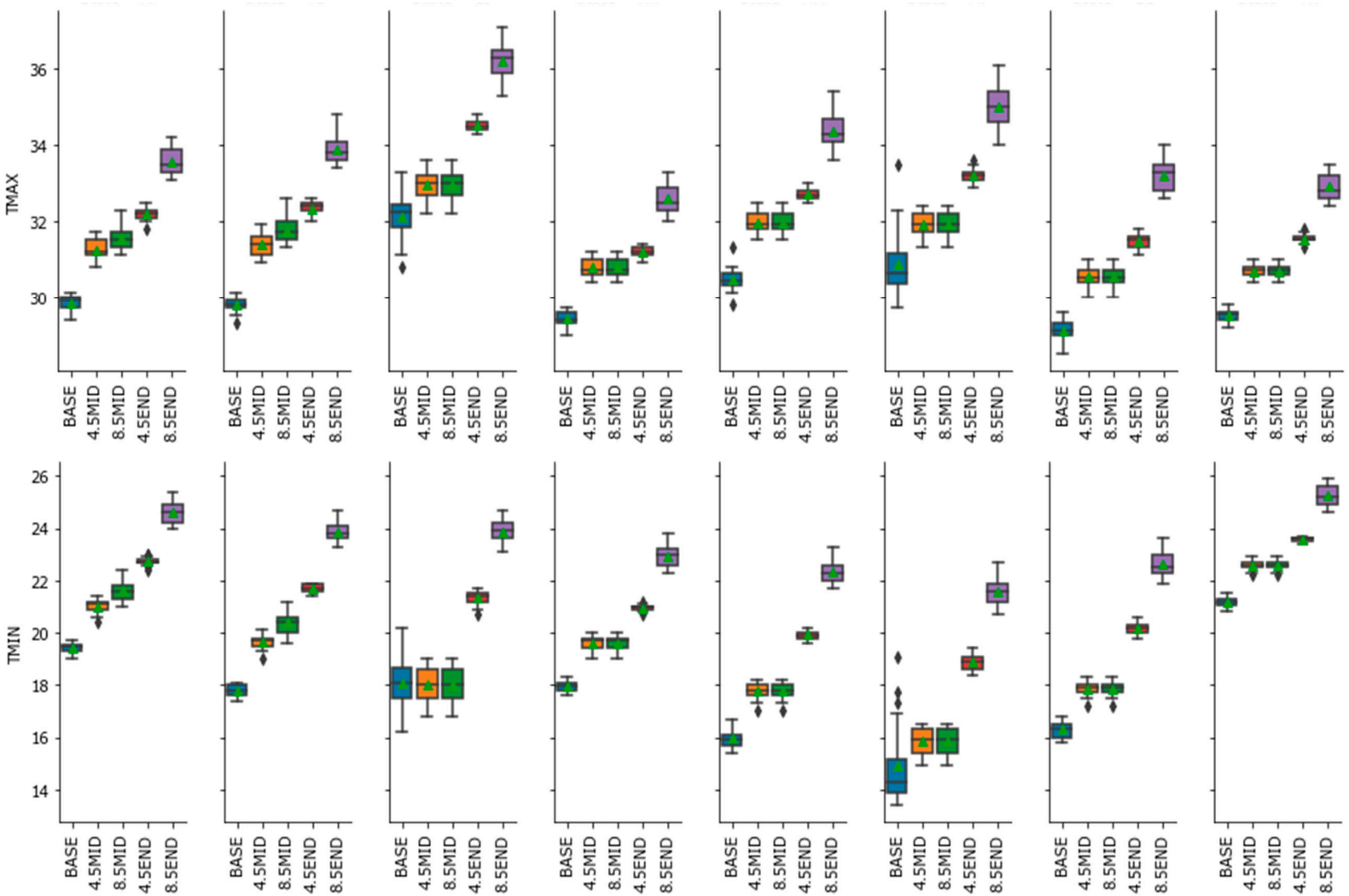

Figure 10. Projected changes in modeled post-rainy season sorghum yields, rainfall amounts, maximum temperatures and minimum temperatures across different time periods and RCPs.

4. Discussion

This paper represents the assessment of future changes in rainfall and temperatures during the northeast monsoon period over the potential sorghum growing regions of India. The statistically downscaled and bias-corrected multi-climate models' projections from the CMIP5 models were used to understand the possible changes in the climate variables and their impacts on *post-rainy* season sorghum growth and yields. The MMM of the NEX-GDDP baseline illustrated the ability of these models to reproduce the historical climate characteristics of the mean and the distribution of rainfall and temperatures. The spatial distribution of the annual, seasonal mean surface temperatures and precipitation distributions agrees well against the IMD gridded data [31,32]. The performance of the MMM-simulated rainfall tended to underestimate the rainfall totals over a complex topography, with the performance of the statistical downscaling largely depending on the historical climate records used. The NEX-GDDP datasets were compared with the Global Meteorological Forcing Dataset (GMFD) for downscaling the near-surface meteorological variables [26]. The fidelity of the MMM simulations over Indian land captured the annual cycle of surface air temperatures, even though there was a cold bias throughout the year. The uncertainties in the NEX-GDDP datasets were due to several factors: (1) the ground-based data (CRU data) could not accurately represent the details of a complex orography due to limited or uneven distribution of the rain gauges; (2) the bias correction was primarily focused on rainy day statistics; and (3) the satellite-estimated datasets such as TRMM (used in bias correction) also contained errors at both the temporal and special scales [33]. Nevertheless, further bias correction using locally relevant datasets (e.g., IMD data) could minimize uncertainties in the current and future ESM and GCM projections.

Projected changes in the mean monsoon rainfall amounts in the near future (2020–2049) and far future (2070–2099) relative to the baseline (1976–2005) indicated an increase of 250–450 mm/season in the SW period and 150–300 mm/season in the NE period. There was a clear consensus among the CMIP5 models about the future projected changes in rainfall amounts over India during the SW and NE monsoon periods. The increase in the rainfall amounts could be attributed to increased intense precipitation events and exaggerated moisture conveyance from the Bay of Bengal into the SPI region, owing to increased warming by the end of the 21st century [34–36]. The MMM of the NEX-GDDP showed around 3.4 degrees of temperature difference by the end of the 21st century during the SW monsoon period and a 3.5-degree increase projected during the NE monsoon period under RCP 8.5.

The CERES-sorghum model was used to simulate the sorghum crops in the Southern Peninsular India (SPI) region using the MMM of the NEX-GDDP climate projections considering two RCPs and periods. The sorghum model performed well in reproducing historic sorghum yields during the *post-rainy* season and matched the reported yields, with R^2 values for the eight states at 0.87 (n = 264, $p < 0.001$). The simulated sorghum yields for the current climate indicate that despite slight overestimation of the grain yield values across the study area, the crop model was able to capture the spatial distribution of the sorghum yields, with a close match for the interannual variability in the reported sorghum yield values. In response to climate change, state-level aggregated mean sorghum yields demonstrated an increase in yields across the study area. The increase in yields followed the south-north dipole of projected rainfall changes. An increase in *post-rainy* season sorghum yields could be attributed to several factors, such as an increase in monsoon and *post-rainy* season rainfall totals, elevated atmospheric CO_2 or an increase in surface temperatures. An increase in rainfall amounts during the *post-rainy* season is thought to be beneficial for sorghum plant growth, with more frequent rainy days [37,38]. The projected climate change scenarios indicate an increase in rainfall amounts as well as an increase in rainy days during the *post-rainy* season. Therefore, the increased rainfall frequency would effectively reduce the intervals between soil moisture stress [39].

The elevated concentrations of CO_2 in response differ by crop type, as there are two crop photosynthesis types: C3 (rice and wheat) and C4 (maize and sorghum). Generally,

the higher atmospheric CO_2 shows much more response to C3 plants than C4 plants. Elevated CO_2 has generally been established to increase crop growth, and in the CERES-sorghum model, elevated concentrations of CO_2 alter crop growth and yields through radiation use efficiency (RUE) and plant transpiration. Under elevated concentrations of CO_2, the CERES-sorghum model applies a multiplier on the RUE, which increases biomass production [40,41]. The response of the CO_2 has interactions with nitrogen fertilizer, and the response is expected to be small for low nitrogen fertilizer amounts. The lesser response to low nitrogen fertilizer amounts is well documented in experiments on rice crops [42,43]. In this study, the nitrogen fertilizer was based on the recommended practices in the region and ranged from 60 to 80 kg ha^{-1}. Higher CO_2 concentrations in the atmosphere are expected to increase biomass production and yields through a large increase in the utilization of available nitrogen [44,45].

The growing evidence suggests that in the tropics and subtropics, crop yields decreased due to warming associated with future climate change. The direct effects of higher surface air temperatures on sorghum crop growth and yields were negative both in controlled environmental studies [46–49] and custom-designed field-based experiments [50,51], which have documented that those high temperatures lead to heat stress in sorghum crops, and during the critical flowering and grain-filling stages, heat stress substantially decreases crop yields. Recent studies have identified a temperature threshold of 33 °C, beyond which sorghum yields start declining [52]. The projected increasing temperatures increase the rate of crop development as well as transpiration. If rainfall amounts are stable or decreasing, then this could lead to water stress and substantially reduce sorghum yields. However, if the rainfall amounts are projected to increase along with the temperatures, then it may be possible to preserve or increase sorghum grain yields. The authors of [50] demonstrated that sorghum crops exposed to short episodes of high temperatures (40–30 °C) during reproductive development could have a significant effect on sorghum yields. In the current study, the future mean maximum temperatures are expected to increase up to 2.1 °C and 3.5 °C during the *post-rainy* season under the RCP 8.5 scenario. The increase in surface air temperatures under the RCP 8.5 scenarios during the *post-rainy* season was still below the optimum temperature threshold, and the mean maximum temperature across the study area varied from 30 °C to 32 °C. Increasing temperatures under climate change scenarios can affect sorghum yields through their influence on water stress [53]. In the present study, it was observed that the rainfall totals during the post-rainy season were increasing under two time periods and RCPs. The increasing rainfall amounts, along with the elevated CO_2 levels in the atmosphere (499 ppm near century, 532 ppm far future under RCP 4.5 and 571 ppm near future and 801 ppm by the end of the 21st century under RCP 8.5) considered in the simulations, increased the sorghum crop yields during the *post-rainy* season.

5. Conclusions

The MMM is often defined as an "ensemble of opportunity" which solves the problem of uncertainties up to some extent that is embodied in the spectrum of future climate change projections. For decision makers, it is of the utmost importance to understand if the level of uncertainty in the future projections remains unchanged or will be considerably reduced in the coming decades. The multi-model approach used in this study was used to demonstrate that combining multiple climate models' projections increases the skill in accurately representing the historical climate and predicting the plausible changes in future climates. The impact assessment community would benefit from the statistically downscaled GCMs projections and intelligently combining multi-model ensembles that could reduce model uncertainty. Further simulating sorghum yields using these multi-model ensemble climate data suggests that the climate change in the region could be an opportunity for the smallholder to adapt and further improve productivity with proper crop management. Global climate change, particularly increases in rainfall amounts, elevated CO_2 levels and future warming (within the optimum range for crop growth and development), allowed sorghum crops during the post-rainy season to sustain increased production. Sorghum crops are

relatively more resilient to harsher environmental conditions, and one reason for this they are often sown under warmer and dry conditions. Our findings suggest that sorghum may indeed be a good crop under climate change in the post-rainy season that is grown under residual soil moisture.

Author Contributions: Conceptualization, K.C. and S.G.; methodology, S.G., K.R.K. and D.M.K.; software, S.G. and K.C.; validation, K.C., K.C.D., K.K.D., R.K.B.D. and S.K.T.; formal analysis, S.G.; investigation, K.C. and S.G.; resources, R.K.B.D. and S.K.T.; data curation, S.G. and D.M.K.; writing—original draft preparation, K.C. and S.G.; writing—review and editing, K.C., S.G., D.M.K., R.K.B.D. and S.K.T.; visualization, S.G.; supervision, S.G.; project administration, S.G.; funding acquisition, S.G. All authors have read and agreed to the published version of the manuscript.

Funding: Authors S Gummadi acknowledges CGIAR Research Program on Climate Change, Agriculture and Food Security (CCAFS), which is carried out with support from the CGIAR Trust Fund.

Institutional Review Board Statement: Not applicable.

Informed Consent Statement: Not applicable.

Data Availability Statement: Not applicable.

Conflicts of Interest: The authors declare no conflict of interest.

References

1. Harlan, J.R.; de Wet, J.M.J. Simplified Classification of Cultivated Sorghum A. *Crop. Sci.* **1972**, *12*, 172–176. [CrossRef]
2. Mundia, C.W.; Secchi, S.; Akamani, K.; Wang, G. A Regional Comparison of Factors Affecting Global Sorghum Production: The Case of North America, Asia and Africa's Sahel. *Sustainability* **2019**, *11*, 2135. [CrossRef]
3. Charyulu, K.D.; Cynthia, B.; Bvs, R.; Ashok, K.A.; Moses, S.D. *Development and Diffusion of Sorghum Improved Cultivars in India: Impact on Growth and Stability in Yield*; Working paper series no. 50; International Crops Research Institute for the Semi-Arid Tropics: Patancheru, India, 2014.
4. GOI. Available online: www.agricoop.nic.in (accessed on 7 June 2021).
5. Kumar, A.A.; Reddy, B.V.S.; Ramaiah, B.; Sahrawat, K.L.; Pfeiffer, W.H. Genetic Variability and Character Association for Grain Iron and Zinc Contents in Sorghum Germplasm Accessions and Commercial Cultivars; Hyderabad. *Eur. J. Plant Sci. Biotechnol.* **2012**, *6*, 1–5.
6. Ashok Kumar, A.; Reddy, B.V.S.; Ramaiah, B.; Sahrawat, K.L.; Pfeiffer, W.H. Gene Effects and Heterosis for Grain Iron and Zinc Concentration in Sorghum [*Sorghum Bicolor* (L.) Moench]. *Field Crops Res.* **2013**, *146*, 86–95. [CrossRef]
7. Pray, C.E.; Nagarajan, L. "Improving Crops for arid Lands": Pearl Millet and Sorghum in India. In *Millions Fed: Proven Successes in Agricultural Development*; Spielman, D.J., Pandya-Lorch, R., Eds.; International Food Policy Research Institute: Washington, DC, USA, 2009; Volume 12, pp. 83–88.
8. Gali, B.; Rao, P.P. Regional Analysis of Household Consumption of Sorghum in Major Sorghum-Producing and Sorghum-Consuming States in India. *Food Secur.* **2012**, *4*, 209–217. [CrossRef]
9. Rao, P.P.; Basavaraj, G.; Ahmad, W.; Bhagavatula, S. An Analysis of Availability and Utilization of Sorghum Grain in India. *J. SAT Agri. Res.* **2010**, *8*, 1–8.
10. Talwar, H.S.; Elangovan, M.; Patil, J.V. (Eds.) Sorghum-A Potential Crop to Adapt to Future Climate Change Scenario. In *Managing Intellectual Property under PVP and PGR*; Directorate of Sorghum Research (DSR): Hyderabad, India, 2013; pp. 254–256.
11. Solomon, S.; Qin, D.; Manning, M.; Chen, Z.; Marquis, M.; Averyt, K.B.; Tignor, M.; Miller, H.L. (Eds.) *Climate Change 2007: The Physical Science Basis: Contribution of Working Group I to the Fourth Assessment Report of the Intergovernmental Panel on Climate Change*; Cambridge University Press: Cambridge, UK, 2007; ISBN 9780521880091.
12. Cline, W.R. (Ed.) *Global Warming and Agriculture: Impact Estimates by Country*; Peterson Institute for International Economics: Washington, DC, USA, 2007.
13. Srivastava, A.; Naresh Kumar, S.; Aggarwal, P.K. Assessment on Vulnerability of Sorghum to Climate Change in India. *Agric. Ecosyst. Environ.* **2010**, *138*, 160–169. [CrossRef]
14. Hengl, T.; de Jesus, J.M.; MacMillan, R.A.; Batjes, N.H.; Heuvelink, G.B.M.; Ribeiro, E.; Samuel-Rosa, A.; Kempen, B.; Leenaars, J.G.B.; Walsh, M.G.; et al. SoilGrids1km—Global Soil Information Based on Automated Mapping. *PLoS ONE* **2014**, *9*, e105992. [CrossRef] [PubMed]
15. Pagire, G.S.; Gadakh, S.R.; Shinde, M.S.; Dalvi, U.S.; Awari, V.R.; Gadakh, S.S. Seasonal Variation in Sowing and Its Effect on Ethanol and Biomass Yield of Sweet Sorghum. *Energy Sources Part A Recovery Util. Environ. Eff.* **2021**, *43*, 716–726. [CrossRef]
16. Trivedi, T.P. (Ed.) *Handbook of Agriculture*; Directorate of Information and Publications of Agriculture, Indian Council of Agricultural Research: New Delhi, India, 2008.
17. Rana, B.S.; Rao, M.H.; Indira, S.; Singh, B.U. *Technology for Increasing Sorghum Production and Value Addition*; Director and Project Coordinator (AICSIP) National Research Centre for Sorghum: Solapur, India, 1999.

18. Hosmani, M.M.; Chittapur, B.M. *Sorghum Production Technology*; University of Agricultural Sciences: Dharwad, India, 1997.
19. Singh, P.; Nedumaran, S.; Traore, P.C.S.; Boote, K.J.; Rattunde, H.F.W.; Prasad, P.V.V.; Singh, N.P.; Srinivas, K.; Bantilan, M.C.S. Quantifying Potential Benefits of Drought and Heat Tolerance in Rainy Season Sorghum for Adapting to Climate Change. *Agric. For. Meteorol.* **2014**, *185*, 37–48. [CrossRef]
20. Sandeep, V.M.; Rao, U.M.v.; Bapuji Rao, B.; Bharathi, G.; Pramod, V.P.; Santhibhushan Chowdary, P.; Patel, N.R.; Mukesh, P.; Vijaya Kumar, P. Sandeep 2018. *J. Agrometeorol.* **2018**, *20*, 89–96.
21. Rajeevan, M.; Unnikrishnan, C.K.; Preethi, B. Evaluation of the ENSEMBLES Multi-Model Seasonal Forecasts of Indian Summer Monsoon Variability. *Clim. Dyn.* **2012**, *38*, 2257–2274. [CrossRef]
22. Lorenz, C.; Portele, T.C.; Laux, P.; Kunstmann, H. Bias-corrected and spatially disaggregated seasonal forecasts: A long-term reference forecast product for the water sector in semi-arid regions. *Earth Syst. Sci. Data* **2021**, *13*, 2701–2722. [CrossRef]
23. Giorgi, F. Simulation of Regional Climate Using a Limited Area Model Nested in a General Circulation Model. *Am. Meteorol. Soc.* **1990**, *3*, 941–963. [CrossRef]
24. Wood, A.W.; Leung, L.R.; Sridhar, V.; Lettenmaier, D.P. Hydrologic implications of dynamical and statistical approaches to downscaling climate model outputs. *Clim. Chang.* **2004**, *62*, 189–216. [CrossRef]
25. Thrasher, B.; Maurer, E.P.; McKellar, C.; Duffy, P.B. Technical Note: Bias Correcting Climate Model Simulated Daily Temperature Extremes with Quantile Mapping. *Hydrol. Earth Syst. Sci.* **2012**, *16*, 3309–3314. [CrossRef]
26. Bao, Y.; Wen, X. Projection of China's near- and Long-Term Climate in a New High-Resolution Daily Downscaled Dataset NEX-GDDP. *J. Meteorol. Res.* **2017**, *31*, 236–249. [CrossRef]
27. White, J.W.; Hoogenboom, G.; Kimball, B.A.; Wall, G.W. Methodologies for Simulating Impacts of Climate Change on Crop Production. *Field Crop. Res.* **2011**, *124*, 357–368. [CrossRef]
28. Jones, J.W.; Hoogenboom, G.; Porter, C.H.; Boote, K.J.; Batchelor, W.D.; Hunt, L.A.; Wilkens, P.W.; Singh, U.; Gijsman, A.J.; Ritchie, J.T. The DSSAT Cropping System Model. *Eur. J. Agron.* **2003**, *18*, 235–265. [CrossRef]
29. Ritchie, I.T. Soil Water Balance and Plant Water Stress. In *Understanding Options for Agricultural Production*; Tsuji, G.Y., Hoogenboom, G., Thornton, P.K., Eds.; Springer Science and Business Media: Berlin/Heidelberg, Germany, 1998.
30. Willmott, C.J.; Ackleson, S.G.; Davis, R.E.; Feddema, J.J.; Klink, K.M.; Legates, D.R.; O'Donnell, J.; Rowe, C.M. Statistics for the Evaluation and Comparison of Models. *J. Geophys. Res.* **1985**, *90*, 8995. [CrossRef]
31. Garnier, P.; Nell, C.; Mary, B.; Lafolie, F. Evaluation of a Nitrogen Transport and Transformation Model in a Bare Soil. *Eur. J. Soil Sci.* **2001**, *52*, 253–268. [CrossRef]
32. Rao, K.K.; Kulkarni, A.; Patwardhan, S.; Kumar, B.V.; Kumar, T.V.L. Future Changes in Precipitation Extremes during Northeast Monsoon over South Peninsular India. *Theor. Appl. Climatol.* **2020**, *142*, 205–217. [CrossRef]
33. Raghavan, S.v.; Hur, J.; Liong, S.Y. Evaluations of NASA NEX-GDDP Data over Southeast Asia: Present and Future Climates. *Clim. Chang.* **2018**, *148*, 503–518. [CrossRef]
34. Sheffield, J.; Goteti, G.; Wood, E.F. Development of a 50-Year High-Resolution Global Dataset of Meteorological Forcings for Land Surface Modeling. *J. Clim.* **2006**, *19*, 3088–3111. [CrossRef]
35. Kitoh, A.; Endo, H.; Krishna Kumar, K.; Cavalcanti, I.F.A.; Goswami, P.; Zhou, T. Monsoons in a Changing World: A Regional Perspective in a Global Context. *J. Geophys. Res. Atmos.* **2013**, *118*, 3053–3065. [CrossRef]
36. Seth, A.; Rauscher, S.A.; Biasutti, M.; Giannini, A.; Camargo, S.J.; Rojas, M. CMIP5 Projected Changes in the Annual Cycle of Precipitation in Monsoon Regions. *J. Clim.* **2013**, *26*, 7328–7351. [CrossRef]
37. Good, S.P.; Caylor, K.K. Climatological Determinants of Woody Cover in Africa. *Proc. Natl. Acad. Sci. USA* **2011**, *108*, 4902–4907. [CrossRef] [PubMed]
38. Guan, K.; Sultan, B.; Biasutti, M.; Baron, C.; Lobell, D.B. What Aspects of Future Rainfall Changes Matter for Crop Yields in West Africa? *Geophys. Res. Lett.* **2015**, *42*, 8001–8010. [CrossRef]
39. Porporato, A.; Daly, E.; Rodriguez-Iturbe, I. Soil water balance and ecosystem response to climate change. *Am. Nat.* **2004**, *164*, 625–632. [CrossRef] [PubMed]
40. Hatfield, J.L.; Boote, K.J.; Kimball, B.A.; Ziska, L.H.; Izaurralde, R.C.; Ort, D.; Thomson, A.M.; Wolfe, D. Climate Impacts on Agriculture: Implications for Crop Production. *Agron. J.* **2011**, *103*, 351–370. [CrossRef]
41. Boote, K.J.; Prasad, V.; Allen, L.H.; Singh, P.; Jones, J.W. Modeling Sensitivity of Grain Yield to Elevated Temperature in the DSSAT Crop Models for Peanut, Soybean, Dry Bean, Chickpea, Sorghum, and Millet. *Eur. J. Agron.* **2018**, *100*, 99–109. [CrossRef]
42. Ziskaac, L.H.; Weerakoona, W.; Pamplonab, R. The Influence of Nitrogen on the Elevated CO_2 Response in Field-Grown Rice. *Aust. J. Plant Physiol.* **1996**, *23*, 45–52.
43. Poorter, H.; Navas, M.-L. Tansley Review Plant Growth and Competition at Elevated CO_2: On Winners, Losers and Functional Groups. *New Phytol.* **2002**, *157*, 175–198. [CrossRef] [PubMed]
44. Torbert, H.A.; Prior, S.A.; Rogers, H.H.; Runion, G.B. Elevated Atmospheric CO_2 Effects on N Fertilization in Grain Sorghum and Soybean. *Field Crop. Res.* **2004**, *88*, 57–67. [CrossRef]
45. Grant, B.; Smith, W.N.; Desjardins, R.; Lemke, R.; Li, C. Estimated N_2O and CO_2 emissions as influenced by agricultural practices in Canada. *Clim. Chang.* **2004**, *65*, 315–332. [CrossRef]
46. Prasad, P.V.V.; Boote, K.J.; Allen, L.H. Adverse High Temperature Effects on Pollen Viability, Seed-Set, Seed Yield and Harvest Index of Grain-Sorghum [*Sorghum Bicolor* (L.) Moench] Are More Severe at Elevated Carbon Dioxide Due to Higher Tissue Temperatures. *Agric. For. Meteorol.* **2006**, *139*, 237–251. [CrossRef]

47. Prasad, P.V.V.; Pisipati, S.R.; Mutava, R.N.; Tuinstra, M.R. Sensitivity of Grain Sorghum to High Temperature Stress during Reproductive Development. *Crop. Sci.* **2008**, *48*, 1911–1917. [CrossRef]
48. Djanaguiraman, M.; Perumal, R.; Jagadish, S.V.K.; Ciampitti, I.A.; Welti, R.; Prasad, P.V.V. Sensitivity of Sorghum Pollen and Pistil to High-Temperature Stress. *Plant Cell Environ.* **2018**, *41*, 1065–1082. [CrossRef] [PubMed]
49. Singh, V.; Nguyen, C.T.; Yang, Z.; Chapman, S.C.; van Oosterom, E.J.; Hammer, G.L. Genotypic Differences in Effects of Short Episodes of High-Temperature Stress during Reproductive Development in Sorghum. *Crop. Sci.* **2016**, *56*, 1561–1572. [CrossRef]
50. Prasad, P.V.V.; Djanaguiraman, M.; Perumal, R.; Ciampitti, I.A. Impact of High Temperature Stress on Floret Fertility and Individual Grain Weight of Grain Sorghum: Sensitive Stages and Thresholds for Temperature and Duration. *Front. Plant Sci.* **2015**, *6*, 820. [CrossRef] [PubMed]
51. Sunoj, V.S.J.; Somayanda, I.M.; Chiluwal, A.; Perumal, R.; Prasad, P.V.V.; Jagadish, S.V.K. Resilience of Pollen and Post-Flowering Response in Diverse Sorghum Genotypes Exposed to Heat Stress under Field Conditions. *Crop. Sci.* **2017**, *57*, 1658–1669. [CrossRef]
52. Tack, J.; Lingenfelser, J.; Jagadish, S.V.K. Disaggregating Sorghum Yield Reductions under Warming Scenarios Exposes Narrow Genetic Diversity in US Breeding Programs. *Proc. Natl. Acad. Sci. USA* **2017**, *114*, 9296–9301. [CrossRef] [PubMed]
53. Lobell, D.B.; Hammer, G.L.; Chenu, K.; Zheng, B.; Mclean, G.; Chapman, S.C. The Shifting Influence of Drought and Heat Stress for Crops in Northeast Australia. *Glob. Chang. Biol.* **2015**, *21*, 4115–4127. [CrossRef] [PubMed]